

Experimental tests of reaction rate theory: $\text{Mu} + \text{H}_2$ and $\text{Mu} + \text{D}_2$

Ivan D. Reid, David M. Garner, Lap. Y. Lee, Masayoshi Senba, Donald J. Arseneau, and Donald G. Fleming

TRIUMF, 4004 Westbrook Mall, Vancouver, British Columbia, V6T 2A3, Canada and Department of Chemistry, University of British Columbia, Vancouver, British Columbia, V6T 1Y6, Canada

(Received 24 December 1986; accepted 12 February 1987)

Bimolecular rate constants for the thermal chemical reactions of muonium (Mu) with hydrogen and deuterium— $\text{Mu} + \text{H}_2 \rightarrow \text{MuH} + \text{H}$ and $\text{Mu} + \text{D}_2 \rightarrow \text{MuD} + \text{D}$ —over the temperature range 473–843 K are reported. The Arrhenius parameters and 1σ uncertainties for the H_2 reaction are $\log A$ ($\text{cm}^3 \text{ molecule}^{-1} \text{ s}^{-1}$) = -9.605 ± 0.074 and $E_a = 13.29 \pm 0.22$ kcal mol^{-1} , while for D_2 the values are -9.67 ± 0.12 and 14.73 ± 0.40 , respectively. These results are significantly more precise than those reported earlier by Garner *et al.* For the Mu reaction with H_2 our results are in excellent agreement with the 3D quantum mechanical calculations of Schatz on the Liu–Siegbahn–Truhlar–Horowitz potential surface, but the data for both reactions compare less favorably with variational transition-state theory, particularly at the lower temperatures.

INTRODUCTION

For over half a century the simplest bimolecular exchange reaction $\text{H} + \text{H}_2$ has held the continuing interest of experimental and theoretical chemists alike. This interest arises from the fact that the H_3 system is still the only reaction for which the potential energy surface is known with sufficient accuracy ($\sim 2\%$)^{1–4} to allow exacting comparisons between theoretical calculations of the reaction dynamics and experimental results. Recent interest in this field has tended to focus on the measurement and calculation of scattering cross sections for isotopic variations of the basis reaction,^{5–11} but measurements of thermal (Boltzmann averaged) reaction rate constants are still important.^{11–15} Such experiments provide the only means of probing the energy regime near threshold, where quantum tunneling effects can be important.

Some of the more interesting isotopic variations of this reaction involve muonium (Mu), a light (0.113 amu) hydrogen-like atom in which the proton is replaced by a positive muon. There have been several theoretical studies,^{10–13,16,17} together with experimental measurements¹⁵ of the thermally averaged reaction rate constants for the isotopic variations



Because of the light muon mass, these reactions are highly endothermic, ΔH_0° being 7.6 and 9.2 kcal mol^{-1} , respectively.¹⁵ As a result, the vibrationally adiabatic barrier is late and zero-point mass effects at the transition-state (TS) dominate the kinetics.

The theoretical treatments for reactions (R1) and (R2) have generally used the Liu–Siegbahn–Truhlar–Horowitz (LSTH) potential energy surface for $\text{H} + \text{H}_2$,^{1–3} although other surfaces such as the Porter–Karplus model have also been considered.^{12,13} It has also been assumed in these studies that the Born–Oppenheimer approximation applies. The treatments have ranged from 1D quantum calculations,^{12,16}

quasiclassical trajectory calculations (QCT),¹⁷ and various flavors of variational transition-state theory^{12,13,17} through to 3D quantum coupled states (CS) calculations.¹¹ It is these last results which are expected¹⁸ to provide the benchmark against which other methods must be compared. For example, while both the improved canonical variation theory (ICVT)^{12,13} results and the CS calculations show agreement, within the considerable experimental uncertainties, with the measurements of Garner *et al.*,¹⁵ there are still significant discrepancies between the CS and ICVT treatments. This is particularly noticeable at temperatures below ~ 608 K, the lowest point measured by Garner *et al.*

Recent developments in H_3 reaction theory include a recalculation of the LS potential energy surface^{3,4} with the result that the potential barrier is now believed to be ~ 0.2 kcal mol^{-1} lower than in the LSTH fit, as well as investigations into the validity of the Born–Oppenheimer approximation^{19,20} which suggest that the true barrier for the $\text{Mu} + \text{H}_2$ reaction may be higher by as much as ~ 0.5 kcal mol^{-1} due to nuclear motion corrections to the potential surface. In parallel with modern advances in theoretical techniques, further and more precise experimental measurements are desirable to aid in the investigation of these subtle effects. Since the original experimental measurements of reactions (R1) and (R2) were conducted, the muon spin relaxation (μSR) technique has been considerably refined due to advances in both muon beam technology and the experimental apparatus used. We report here further measurements of reaction rate constants for these reactions, over a wider temperature range and with increased experimental precision, representing an attempt to provide more exacting comparisons with the various theoretical treatments.

EXPERIMENTAL

The μSR technique, which has been developed into a routine method for investigating a variety of chemical and physical phenomena, is extensively described elsewhere (e.g., Walker,²¹ and references therein) and for the sake of

brevity will not be discussed in detail here. For the present experiments an external magnetic field of ~ 4 G was applied to a high-pressure vessel containing the gas reagent and histograms of muon decay events were obtained from decay-positron detectors placed above and below the vessel. Exponential relaxation of the coherent muonium precession signal (~ 6 MHz) is attributed to chemical reactions which occur at random times, placing the muon into a diamagnetic environment (e.g., MuH) where it precesses at a much slower rate (~ 60 kHz). By measuring the relaxation rate λ of the muonium signal as a function of the reactant concentration $[\text{X}]$, one can arrive at a value for the thermally averaged bimolecular reaction rate constant k , through the relation²¹

$$\lambda([\text{X}]) = \lambda(0) + k[\text{X}], \quad (1)$$

where $\lambda(0)$ is the residual relaxation rate measured in the absence of any reactant.

Because of the low rate constants and high activation energies of reactions (R1) and (R2), high reactant concentrations (i.e., pressures), and temperatures must be used to produce an observable relaxation in the muonium signal during the $2.2 \mu\text{s}$ muon radioactive lifetime. To accommodate these pressures and temperatures, a new reaction vessel was built for the present experiments. The design goals for this vessel were 10 000 Torr at 500 K, and 5000 Torr at 900 K, providing a worthwhile increase in performance over the previous experiment. Constraints imposed by the μSR technique upon the design of reaction vessels include the follow-

ing: (a) All construction materials must be nonmagnetic; (b) the mass thickness of the muon entrance path must be less than the "surface" muon²² range of $\sim 140 \text{ mg cm}^{-2}$ —this includes the incident particle detector, beamline windows, air gaps and, in our case, insulation and heat shielding; (c) the vessel walls must be thin enough to be transparent to muon decay positrons with energies from ~ 35 to 52.8 MeV; (d) the reaction vessel must be large enough to encompass the muon stopping distribution and minimize the diamagnetic "wall signal" arising from muons stopping in the reaction vessel walls, rather than the gas, through range straggling and multiple scattering at the entrance window; and (e) the outer surface of the vessel must remain at a temperature below $\sim 100^\circ\text{C}$ to avoid heat damage to the plastic scintillator particle detectors.

The main obstacle presented by these constraints was the design of a suitable entrance window, especially since the strength of most suitable materials decreases substantially at elevated temperatures. We selected a foil of Inconel alloy, 0.05 mm thick, formed under hydrostatic pressures at 5.5 MPa into a 2.0 cm diam dome, which was then welded to a stainless-steel carrier. The reaction vessel itself (Fig. 1) was made from 316 stainless steel, 25 cm in diameter and 64 cm long with 3.2 mm thick walls. This was enclosed in a vacuum jacket of similar construction to provide thermal insulation. Several copper and aluminum heat shields in the vacuum space minimized radiative heat loss. The window in the outer vessel was 0.05 mm aluminized Mylar, while the heat shields within the beam path were 0.0125 mm thick.

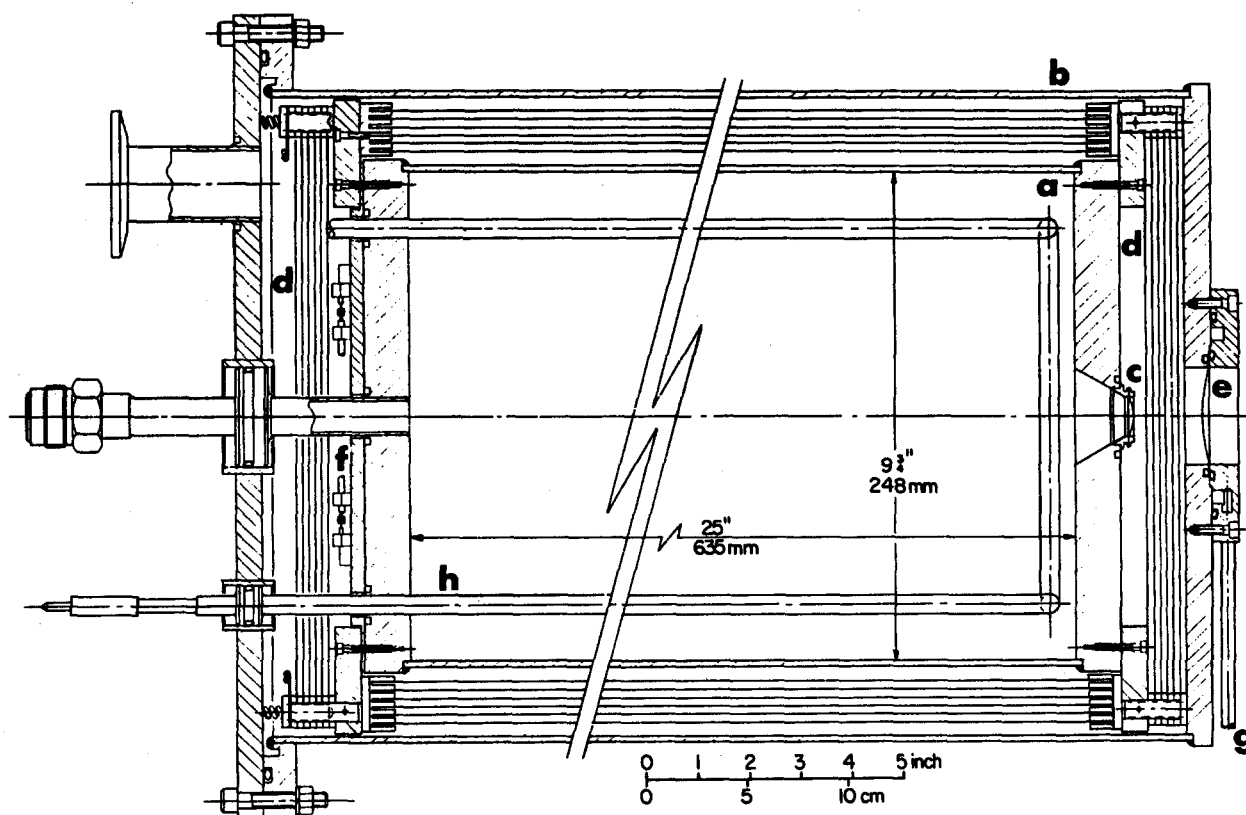


FIG. 1. The high-pressure, high-temperature muonium reaction vessel used in this work. (a) Inner pressure vessel; (b) outer vacuum jacket; (c) Inconel muon entrance window; (d) heat shields; (e) aluminized Mylar outer window; (f) heater plate; (g) outer window coolant; (h) thermocouple tube to monitor gas temperature.

The reaction vessel was heated electrically at one end, originally by Thermocoax elements silver-soldered into a 6 mm copper plate. However, this design proved to be fragile and failed before many experiments could be conducted.²³ For the bulk of the experiments the original heater was replaced with two spiral-wound Chromalox TEBI-170-10 (60 V/500 W) heating elements, soldered to a 1.5 mm copper plate. Type J thermocouples (Omega Engineering, Inc.) were used to monitor the temperatures of the heater plate and the end plate of the reaction vessel. The gas temperature was measured by further thermocouples placed at varying locations along a thin stainless-steel tube within the reactor volume. The power input required to maintain the gas temperature at 850 K was approximately 600 W. Before the experiment was attempted the vessel was required to pass safety tests at full temperature and twice the working pressure.

Unlike the previous design,¹⁵ the present reaction vessel was planned to minimize the temperature gradient along its length. Although it did not perform as well as expected in this regard, we nevertheless achieved a significant improvement over the earlier vessel. Most of the temperature variation occurred at the heater to end plate and end plate to gas interfaces, implying relatively large thermal resistances at these points. Because of limitations on the heater temperature, the gradient along the reaction vessel restricted the maximum gas temperature to 850 K. There was also a considerable vertical temperature gradient, with a typical temperature difference of 8° to 10° between the top and bottom thermocouple tubes. During the experiments the temperature of the heater plate was controlled to maintain a stable gas temperature, monitored at a fixed point, within $\pm 2^\circ$ of a given nominal value. At the completion of experiments at each temperature the horizontal temperature distribution in both top and bottom thermocouple tubes was measured to obtain the average temperature and variation across the muon stopping distribution. The uncertainties in the temperature was found to vary from 4° at 473 K to 14° at 843 K, compared to an estimated variation of ± 25 K at all temperatures in the earlier experiments.

The design of the reaction vessel paid particular attention to eliminating sources of uncertainty in the earlier measurements.¹⁵ The major source of uncertainty in these results was large values of $\lambda(0)$, often comparable to or greater than the measurable variation in $\lambda([X])$. These high values arose from inhomogeneities in the applied magnetic field resulting first from the use of Helmholtz coils which were small relative to the size of the muon stopping distribution, and second from the magnetic fields produced by the electrical heaters placed around the center of the reaction vessel. The counter-wound design of the heaters in the present vessel, and their placement distance from the muon stopping region has effectively eliminated any stray magnetic field from this source—measurements of $\lambda(0)$ in pure argon showed no discernable difference between experiments when the heater was operating and those when it was off during cooling. As well, a new set of 1.5 m diam Helmholtz coils, which produces a field homogeneous to 0.1% over a volume of 10 l, has been in use in this laboratory for a number of years now and has greatly

reduced the inhomogeneities over that of the previously used 60 cm pair.

As far as improvements in beam technology are concerned, the greatest impact has been from the availability of more intense muon beams which, together with improvements in our detectors and electronics, allow a much higher number of counts to be accumulated in a reasonable time, with a concomitant reduction in the statistical uncertainties. For this work, typically two million or more muon decay events were recorded in each histogram for each experiment, which took approximately 1 h, compared to the several hundred thousand events per histogram accumulated in the previous work. The improved beam configuration now available also had a major impact in the design of the reaction vessel, allowing us to use a much smaller and therefore much stronger entrance window. Thus it was not necessary to include any window support such as used previously with a deleterious effect¹⁵ on the incident muon rate and background signal. The use of dc separators²⁴ to eliminate beam positron contamination has also improved matters over the former situation where the window support scattered this contamination into the positron detectors and caused a high time-dependent background. In the current experiments, the measured background was usually less than 1% and showed no evidence of any time structure.

The present experiments were conducted on the new M15 surface muon channel at TRIUMF.²⁵ Because of the thickness of the windows and heat shields, muons with a slightly higher momentum than surface muons, ~ 31 MeV/c, were required to penetrate into the inner volume, while low density gas charges, equivalent to ~ 400 Torr of Ar at 273 K, were needed to obtain a suitable stopped muon distribution. The reaction samples consisted of UHP Ar (Linde, 99.999% purity) and UHP H_2 (Matheson, 99.999% purity) or CP D_2 (Canadian Liquid Air and Matheson, 99.6% purity), introduced in proportions calculated to maintain a constant muon stopping power (i.e., constant electron density) at each temperature. Pressures of the gas mixtures were measured by digital readout from an MKS 221A-10000 pressure transducer with a stated accuracy of 0.5%, a small improvement over the Matheson test gauge used earlier, which had a typical accuracy of 1%. The argon was used without further purification, while the hydrogen and deuterium were introduced through a zeolite trap cooled with liquid nitrogen.

Typically, three or four reactant concentrations were used at each temperature, while on a few occasions only two concentrations [in addition to $\lambda(0)$ runs] were studied due to the pressures of limited beam time. Measurements of $\lambda(0)$ were made in pure argon at each temperature, when experimental conditions allowed stable temperatures to be attained before beam was delivered to the experiment, or during the time taken to change from one temperature to the next. Values obtained for $\lambda(0)$ were found to be relatively insensitive to variation in the density of the gas charge [e.g., $\lambda(0) = 0.03 \pm 0.01 \mu\text{s}^{-1}$ for 1020 Torr Ar and $0.06 \pm 0.005 \mu\text{s}^{-1}$ for 800 Torr Ar at 598 K, cf $\lambda = 0.48 \pm 0.04 \mu\text{s}^{-1}$ for 7800 Torr of H_2 at that temperature] and showed a slight increase with temperature ($0.04 \pm 0.005 \mu\text{s}^{-1}$ at 500

K vs $0.08 \pm 0.01 \mu\text{s}^{-1}$ at 704 K for equal Ar densities).

RESULTS

The thermal bimolecular rate constants were obtained by a simultaneous fit to Eq. (1) of the relaxation rates from the independent top and bottom histograms. A typical plot of relaxation rate (λ) as a function of reactant concentration is shown in Fig. 2. It should be noted that the Mu atom formed in our experiments thermalizes on a nanosecond time scale,²⁶ so that it is in thermal equilibrium with the gas at reaction times of $\sim 1 \mu\text{s}$ (Fig. 2). Figure 2 shows data obtained at 609 K, illustrating the ease with which we were able to measure the difference $\lambda([X]) - \lambda(0)$ at this temperature. This was the lowest temperature point reported in the earlier data for (R1)¹⁵ and was accompanied by an estimated uncertainty of $\sim 150\%$. The greatly reduced values of $\lambda(0)$ and uncertainties in the present experiment have allowed us not only to improve the precision of our results, but also to extend the experiments to much lower temperatures—the lower limit occurs where the measurable variation in λ with concentration approaches the uncertainties in its measurement.

The overall rate constants are given in Table I and illustrated in Fig. 3 as Arrhenius plots. Figure 3 also includes the theoretical predictions from the ICVT calculations with a least active ground state tunneling path (LAG)¹³ for reactions (R1) and (R2), along with the CS¹¹ results for reaction (R1). The given temperature uncertainties are the measured gradients, while the (1σ) uncertainties in the rate constants arise primarily from counting statistics, via uncertainties in the fitted values for relaxation rates from the data

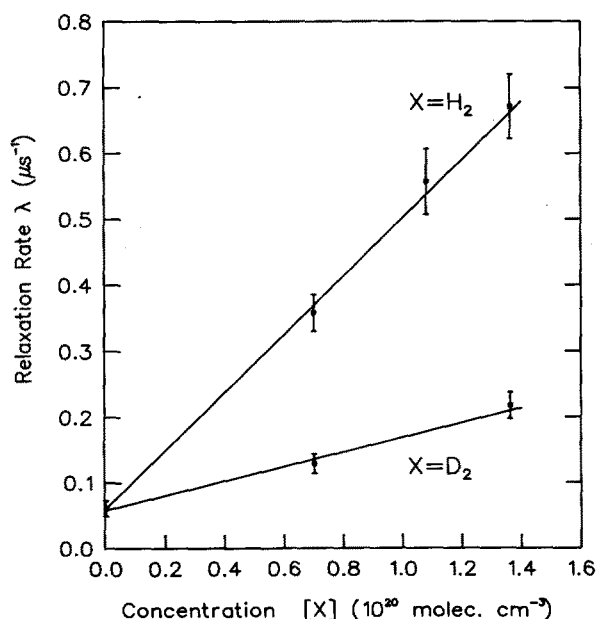


FIG. 2. Relaxation rate λ as a function of reactant concentration for reactions (R1) and (R2) at 609 K. For clarity, the values of λ shown are averages of the results obtained from the top and bottom detectors. The straight lines are fits of Eq. (1) to the data, yielding the bimolecular reaction rate constants (Table I).

TABLE I. Experimental bimolecular rate constants for reactions (R1) and (R2).

	$T(\text{K})$	k ($10^{-14} \text{ cm}^3 \text{ molecule}^{-1} \text{ s}^{-1}$)
Mu + H ₂ (R1)	843 ± 14	9.53 ± 0.51
	794 ± 11	5.23 ± 0.28
	749 ± 10	3.33 ± 0.18
	704 ± 9	2.027 ± 0.085
	669 ± 9	1.136 ± 0.053
	650 ± 9	0.787 ± 0.026
	609 ± 9	0.441 ± 0.018
	598 ± 6	0.311 ± 0.013
	576 ± 6	0.210 ± 0.010
	558 ± 7	0.177 ± 0.011
	538 ± 7	0.1052 ± 0.0060
	500 ± 4	0.0493 ± 0.0056
	498 ± 5	0.0376 ± 0.0070
473 ± 4	0.0150 ± 0.0054	
Mu + D ₂ (R2)	843 ± 14	3.26 ± 0.14
	794 ± 11	1.976 ± 0.086
	749 ± 10	1.013 ± 0.050
	704 ± 9	0.555 ± 0.021
	669 ± 9	0.381 ± 0.019
	650 ± 9	0.2068 ± 0.0090
	609 ± 9	0.111 ± 0.011
	598 ± 6	0.0950 ± 0.0068

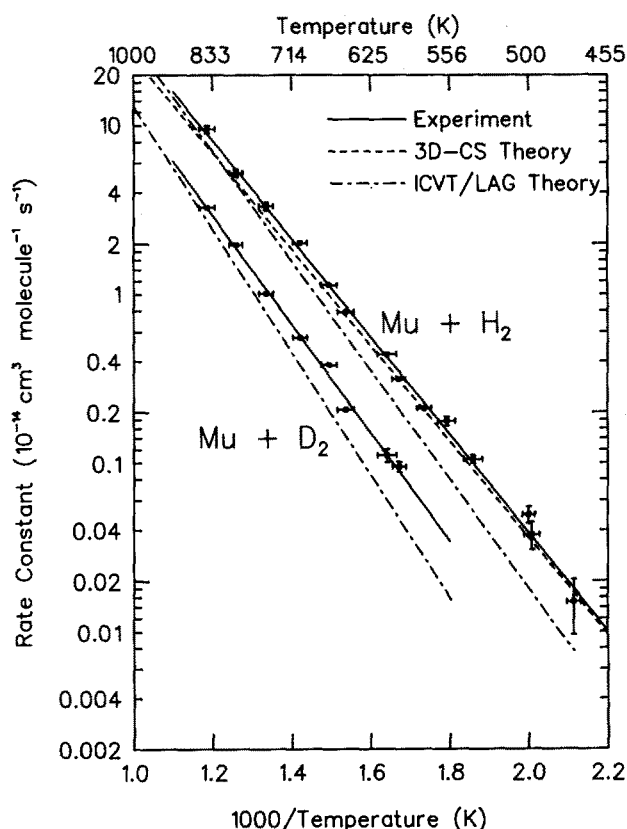


FIG. 3. Experimental measurements and theoretical predictions of the reaction rate constants for reactions (R1) and (R2). Points and solid lines—this experiment; dashed line—3D CS theory (Ref. 11); dot-dash line—ICVT/LAG theory (Ref. 13).

histograms. The rate constants were fitted to the usual Arrhenius expression $k = A \exp(-E_a/RT)$, using the method of Cvetanovic and Singleton²⁷ to obtain the exact statistical weighting of $\ln k$, yielding the Arrhenius parameters presented in Table II. These parameters all lie within the quoted uncertainties of Garner *et al.*¹⁵ However, it should be noted that preliminary values of the Arrhenius parameters for both reactions,²³ calculated from a small subset of the present reaction rate constants together with some data gathered under conditions of poor temperature stability plus the results of Garner *et al.*, show some significant differences from the final values given here.

DISCUSSION

From Fig. 3 it is immediately apparent that we have succeeded in our goal of improving the precision of experimental values of the rate constants for reactions (R1) and (R2) to the point where the most recent theoretical treatments can be tested effectively. Unfortunately, there are presently no CS calculations for the deuterium reaction (R2) but the results of Schatz¹¹ for the hydrogen reaction (R1) lie extremely close to our Arrhenius fit, in all cases within the 30% accuracy claimed for the CS results (e.g. -17% at 843 K and -8% at 473 K). As well, Schatz's quoted activation energy of $13.0 \text{ kcal mol}^{-1}$ (Table II) is barely outside our estimated uncertainty, so the discrepancies cannot be regarded as highly significant. This experimental verification of the most accurate calculation to date for reaction (R1) is an important test of reaction theory. In addition, it now provides the incentive for a full coupled channels (CC) treatment of this reaction, together with reaction (R2) if possible. Such a CC treatment would eliminate the $\sim 30\%$ uncertainty associated with the CS method and provide further tests of its relative accuracy over a wide range of isotopic mass. More importantly perhaps, a CC calculation would also allow definitive statements to be made about the adequacy of the Born–Oppenheimer approximation,^{19,20} and provide the opportunity to investigate the effect of recent small corrections to the LS barrier height.^{3,4}

However, it seems clear that the intrinsic accuracy of the LSTH surface is confirmed by the level of agreement noted above. The overall accuracy of this surface is also well established from other isotopic reactions on the ground state

($v = 0$) of H_2 , but there has been continuing discussion in the literature as to its accuracy for the same reactions on $\text{H}_2^*(v = 1)$ in the face of a considerable level of disagreement between theory and experiment.^{10,14,28–30} The present Mu results tend to confirm recent statements that the LSTH surface itself is not the cause of this disagreement^{3,10,11,29,30} since reactions (R1) and (R2), being so endothermic, tend to probe the same region of the surface as do other reactions on $\text{H}_2^*(v = 1)$. Note that the thermal populations of the $\text{H}_2^*(v = 1)$ state is $\leq 0.2\%$, even at 1000 K.

In contrast with the excellent agreement obtained between the CS method and the experimental results for reaction (R1), the ICVT/LAG results of Garrett and Truhlar¹³ for both reactions (R1) and (R2) lie significantly outside the experimental uncertainties at the lower temperatures while agreeing well with our data at the highest temperatures. This trend is reflected in the activation energies shown in Table II as well as in the ratios of the reaction rates (R1)/(R2) given in Table III for selected temperatures. The ICVT/LAG activation energies presented in Table II were calculated from the theoretical reaction rates over the temperature range 400–845 K,¹³ assuming the activation energies to be temperature independent. In fact, the LAG results do show some temperature dependence but nevertheless the calculated activation energies are significantly higher than the experimental values at all temperatures. The kinetic isotope effects given in Table III from extrapolations of our Arrhenius parameters and for the ICVT/LAG results exhibit a similar behavior: at the highest temperature (1000 K) the agreement with the experimental ratio is very good, but at 300 K the LAG ratio is noticeably higher than the experimental value.

From these comparisons, we conclude that the ICVT/LAG calculations are a less accurate description of the reaction than the CS method. These two techniques have also been compared by Schatz^{10,11} for reaction (R1) as well as by Garrett *et al.* for other reactive systems.¹⁸ Generally, the ICVT/LAG calculations agree with the CS results, typically to better than 10%. However, the LAG treatment of quantum tunneling is not expected to be as accurate as the MCPSAG or MCPVAG methods,^{12,13,18} a failing which is most likely to be manifest in studies of Mu reactivity.¹⁵ Indeed, the ICVT/MCPSAG calculations reported by Garrett and Truhlar for reaction (R1)¹³ do lie slightly closer to the present experiment at the lowest temperatures than the LAG results, but they still fall significantly below the excellent agreement seen for the CS results. On the other hand, there is virtually no difference between the LAG and SAG

TABLE II. Arrhenius parameters for reactions (R1) and (R2) obtained in this work, compared to those of Garner *et al.* (Ref. 15) and to CS (Ref. 11) and ICVT/LAG (Ref. 13) theories (see the text). Uncertainties are (1σ) .

	$\log A \text{ (cm}^3 \text{ molecule}^{-1} \text{ s}^{-1}\text{)}$	$E_a \text{ (kcal mol}^{-1}\text{)}$
Mu + H₂		
This expt.	-9.605 ± 0.074	13.29 ± 0.22
Garner <i>et al.</i>	$-9.62^{+0.47}_{-0.43}$	$13.8^{+1.6}_{-1.5}$
CS theory		13.0
ICVT/LAG theory		14.4
Mu + D₂		
This expt.	-9.67 ± 0.12	14.73 ± 0.40
Garner <i>et al.</i>	$-9.17^{+1.31}_{-0.99}$	$17.2^{+4.9}_{-3.5}$
ICVT/LAG theory		16.2

TABLE III. Comparison of kinetic isotope effects between experiment and ICVT/LAG calculations (Ref. 13).

$T(\text{K})$	(R1)/R2	(R1)/R2
	This expt.	ICVT/LAG
400	7.1 ± 2.5	9.8
600	3.9 ± 0.3	4.3
1000	2.4 ± 0.3	2.4

results for reaction (R2), which is consistent with the claim¹¹ that the ICVT methods do not accurately describe “deep” quantum tunneling—in these late barrier reactions, the reduced mass for reaction (R2) is twice that for reaction (R1).¹⁵

Finally, a close study of Fig. 3 reveals that the present apparatus could be used to extend the measurements in D_2 down to about 530 K. However, this was not possible during the course of the present investigation due to shortages of both beam time and deuterium gas. Extrapolating our data to 400 K and stipulating a range of $0.1 \mu\text{s}^{-1}$ in the observed muonium relaxation rates predicts that pressures up to 400 atm will be required to measure reaction (R1) at this temperature—reaction (R2) would require a further factor of 7. Fortunately, the much higher muon stopping densities at these pressures would allow the use of smaller reaction vessels, although the strength of materials required to contain the reactant would dictate the use of higher energy “backward” muons in order to penetrate into the sample volume. Reaction vessels with similar design parameters have been used in μSR studies in liquid chemistry,³¹ so it is possible that future experimental studies of these reactions could be carried out at lower temperatures. Motivation for this additional experimental effort, however, must arise from developments in theory since without a more accurate (CC) treatment it is not clear that this endeavour would shed more light on reaction dynamics. It should also be noted here that there is, unfortunately, no foreseeable prospect of measuring the state resolved cross sections calculated by Schatz^{10,11}

ACKNOWLEDGMENTS

We would like to acknowledge the contributions made by R. Blaby and R. Gadd in the design of the reaction vessel, and by K. Hoyle and J. Worden in its fabrication, assembly, and testing. The financial assistance of NSERC (Canada) is gratefully acknowledged. We would also like to thank the Petroleum Research Foundation of the American Chemical Society for its financial support.

- ¹P. Siegbahn and B. Liu, *J. Chem. Phys.* **68**, 1794 (1978).
- ²D. G. Truhlar and C. J. Horowitz, *J. Chem. Phys.* **68**, 2446 (1978).
- ³M. R. A. Blomberg and B. Liu, *J. Chem. Phys.* **82**, 1050 (1985).
- ⁴B. Liu, *J. Chem. Phys.* **80**, 581 (1984).
- ⁵F. Webster and J. C. Light, *J. Chem. Phys.* **85**, 4744 (1986).
- ⁶N. C. Blais, D. G. Truhlar, and B. C. Garrett, *J. Chem. Phys.* **82**, 2300 (1985).
- ⁷K. Tsukiyama, B. Katz, and R. Bersohn, *J. Chem. Phys.* **84**, 1934 (1986).
- ⁸D. P. Gerrity and J. J. Valentini, *J. Chem. Phys.* **83**, 2207 (1985).
- ⁹E. E. Marinero, C. T. Rettner, and R. N. Zare, *J. Chem. Phys.* **80**, 4142 (1984).
- ¹⁰G. C. Schatz, in *Theory of Chemical Reaction Dynamics*, edited by D. Clary, NATO Workshop (Riedel, Dordrecht, 1986), p. 1.
- ¹¹G. C. Schatz, *J. Chem. Phys.* **83**, 3441 (1985).
- ¹²D. K. Bondi, D. C. Clary, J. N. L. Connor, B. C. Garrett, and D. G. Truhlar, *J. Chem. Phys.* **76**, 4986 (1982).
- ¹³B. C. Garrett and D. G. Truhlar, *J. Chem. Phys.* **81**, 309 (1984).
- ¹⁴N. AbuSalbi, D. J. Kouri, Y. Shima, and M. Baer, *J. Chem. Phys.* **82**, 2650 (1985).
- ¹⁵D. M. Garner, D. G. Fleming, and R. J. Mikula, *Chem. Phys. Lett.* **121**, 80 (1985).
- ¹⁶J. N. L. Connor, *Hyperfine Interact.* **8**, 423 (1981).
- ¹⁷N. C. Blais, D. G. Truhlar, and B. C. Garrett, *J. Chem. Phys.* **78**, 2363 (1983).
- ¹⁸B. C. Garrett, D. G. Truhlar, and G. C. Schatz, *J. Am. Chem. Soc.* **108**, 2876 (1986).
- ¹⁹B. C. Garrett, D. G. Truhlar, *J. Chem. Phys.* **82**, 4543 (1985); **84**, 7057 (1986).
- ²⁰N. C. Handy, T. J. Lee, and W. H. Miller, *Chem. Phys. Lett.* **125**, 12 (1986).
- ²¹D. C. Walker, *Muon and Muonium Chemistry* (Cambridge University, Cambridge, 1983).
- ²²A. E. Pifer, T. Bowen, and K. R. Kendall, *Nucl. Instrum. Methods* **135**, 39 (1976).
- ²³I. D. Reid, L. Y. Lee, D. M. Garner, D. J. Arseneau, M. Senba, and D. G. Fleming, *Hyperfine Interact.* **32**, 801 (1986).
- ²⁴J. L. Beveridge, J. Doornbos, D. M. Garner, D. J. Arseneau, I. D. Reid, and M. Senba, *Nucl. Instrum. Methods A* **240**, 316 (1985).
- ²⁵J. L. Beveridge, J. Doornbos, and D. M. Garner, *Hyperfine Interactions*, **32**, 907 (1986).
- ²⁶D. G. Fleming, R. J. Mikula, and D. M. Garner, *Phys. Rev. A* **26**, 2527 (1982).
- ²⁷R. J. Cvetanovic and D. L. Singleton, *Intern. J. Chem. Kinet.* **9**, 481, 1007 (1977).
- ²⁸V. B. Rozenshtein, Yu. M. Gershenzon, A. V. Ivanov, S. D. Il'in, S. I. Kucheryavii, and S. Ya. Umanskii, *Chem. Phys. Lett.* **121**, 89 (1985).
- ²⁹B. C. Garrett and D. G. Truhlar, *J. Phys. Chem.* **89**, 2204 (1985).
- ³⁰E. Pollak, N. AbuSalbi, and D. J. Kouri, *Chem. Phys. Lett.* **113**, 585 (1985).
- ³¹K. E. Newman, *Rev. Sci. Instrum.* **56**, 1470 (1985).